JOURNAL OF MATERIALS SCIENCE **37** (2002) 5371 – 5379

Microstructure and creep properties of a cast Mg-1.7%wt rare earth-0.3%wt Mn alloy

D. WEISS
DSM Ltd., Israel

A. A. KAYA
Ben-Gurion University of The Negev, Department of Materials Sci. & Eng., Beer-Sheva, Israel

E. AGHION
DSM Ltd., Israel

D. ELIEZER
Ben-Gurion University of The Negev, Department of Materials Sci. & Eng., Beer-Sheva, Israel

A study has been undertaken to reveal the creep properties of an experimental magnesium alloy, Mg-1.7RE-0.3Mn, and its microstructure after creep. Transmission electron microscopy examinations on the samples over aged during creep showed that extensive precipitation of $Mg_{12}RE$ type intermetallics took place on dislocations in the form of long single rows. Other precipitates of $Mg_{12}RE$ with lozenge morphology were observed to be distributed more uniformly inside the grains. Precipitates types have been identified via X-ray and electron diffraction, and microanalysis techniques. The relatively low creep rate compared to the commercial magnesium alloys was measured. A high value of activation energy, 240 kJ/mol, was calculated. The creep resistance and the activation energy of the alloy were discussed in terms of microstructural observations.

1. Introduction

The use of light weight magnesium alloy parts in the transportation industry for applications exposed to elevated temperatures has been limited by the inferior creep resistance of the standard die castable alloys of magnesium. It has been known that addition of rare earth elements such as Ce, Nd, La and Pr to magnesium alloys has a beneficial effect on the creep resistance.

The as-cast microstructure of Mg-RE alloys consists of Mg α grains surrounded by coarse $Mg_{12}RE$ intermetallic precipitates. The solubility of RE elements in magnesium is very limited, Ce and Nd having the highest solubility limit of 0.09 at% [1]. Since the solubilities of RE elements rapidly decreases with temperature the alloys belonging to Mg-RE system responses to aging. L. Y. Wei *et al.* [2] and M. Hisha [3], previously studied alloy compositions based on Mg-Ce, and reported that precipitation processes are complex and involve a sequence of stages. It was shown that the first precipitate to form was β'' with a stepped DO19 crystal structure which transformed into β' of DO19 crystal structure. The last stage of the transformation was the β phase formation. This transition took place in the over aged condition. The equilibrium precipitate, β, has a body centered tetragonal $Mg_{12}RE$ structure.

The effect of Mn on the Mg-RE system was studied by Leontis *et al.* [4] and Mellor [5]. Their findings indicated that the addition of Mn tended to alter the creep resistance by reducing the size and increasing the amount of the precipitates.

The objective of this research was to study the effect of Rare Earth and Mn on the microstructure and creep Properties of a cast high temperature magnesium alloy.

2. Experimental procedure

The alloy was prepared in an electric resistance furnace of 10 kg capacity at 700 °C under a protective atmosphere of dry air and 0.6 vol% SF_6 gas mixture, and cast into permanent molds. Rare earth addition was made in the form of Ce-enriched mischmetal. The alloy was solution treated at 560 °C for 8 hours under a protective atmosphere and water quenched to room temperature. A subsequent ageing treatment was performed at 200 °C.The chemical composition of the alloy is given in Table I.

Samples for Scanning Electron Microscopy (SEM) were polished in the conventional way and etched with 5% HNO_3 solution. Thin foils for Transmition Electron Microscopy (TEM) were prepared by mechanical polishing followed by electropolishing using an electrolyte mixture of 60% methanol, 35% butanol and 5% perchloric acid at 15 V and at −40 °C. SEM was conducted with a JEOL 840 operating at 10 kV. TEM was performed using a JEOL 2010 operating at 200 kV.

Rigako D2000 type machine was used for X-ray diffraction using Cu Kα 140 kV, 30 mA radiation.

Vickers microhardness measurements were made by using 10 g load, and an average of 5 measurements were taken in each case. The compression tests were performed on an Instron 4483 type machine. Creep tests were conducted on a SATEC creep machine under a stress range of 50 to 60 MPa and at a temperature range of 190–210°C.

TABLE I Chemical composition of the alloy MG 1.7RE(Ce)0.3Mn

	Mn	Ce	La	Nd	Pr
%wt	0.28	0.88	0.5	0.31	0.05

3. Results—Microstructure

The microstructures of the as-cast, solution treated and aged (under creep) are presented in Fig. 1. The as-cast and solution treated conditions appear similar, being composed of α Mg matrix and $Mg_{12}RE$ type intermetallic precipitates decorating the dendrite boundaries. However, the volume fraction of particles decreases in the order of as-cast (8%), solution treated (4%) and solution treated and crept samples (4%). Due to the low solubility limits of RE elements $Mg_{12}RE$ type precipitates persist to be present even after solution treatment.

X-ray diffraction spectra of the as-cast and solution treated condition are presented in Fig. 2a and b. The X-ray diffraction spectra confirmed the presence of

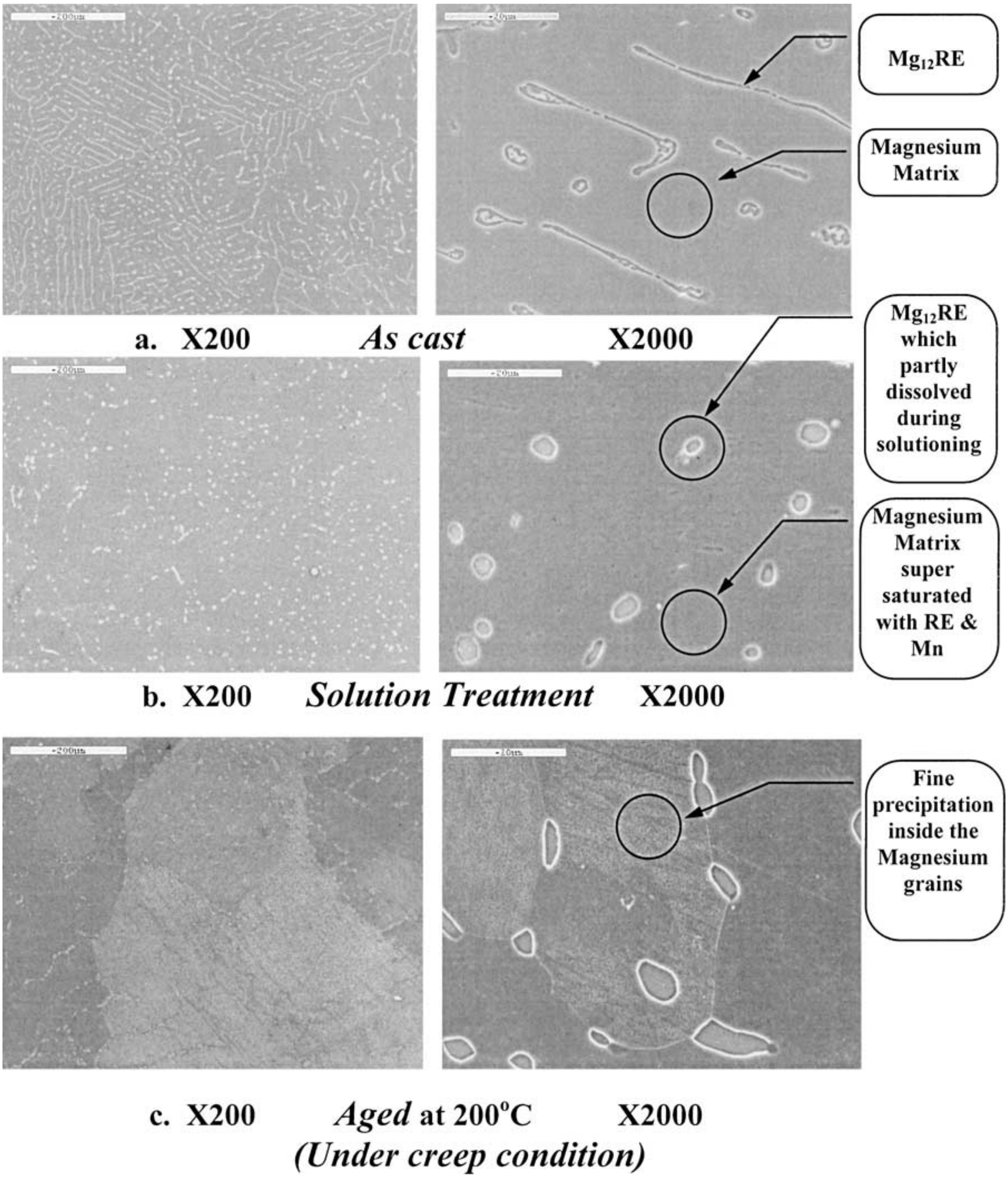

a. X200 *As cast* X2000

b. X200 *Solution Treatment* X2000

c. X200 *Aged* at 200°C X2000 *(Under creep condition)*

Figure 1 Alloy Mg-1.7 RE-0.3Mn–In the (a) Cast, (b) Solutioned and (c) Aged conditions.

$Mg_{12}Ce$ and $Mg_{12}Nd$ type precipitates in the as cast and solution conditions as shown. Further details of the aged under creep microstructure were revealed by high magnification SEM and TEM examinations. Fine intermetallic precipitates were observed in the aged material as shown in Fig. 3a and b . It was also observed (Fig. 3a) that precipitate-free zones along the grain boundaries exist in the crept sample.

Fig. 3c indicated that creep failure initiated at the phase boundaries between the grain boundary coarse precipitates and the matrix particularly on grain boundaries lying perpendicular to the applied stress. Internal cracking was common in these coarse precipitates (Fig. 3b) possibly occurring before the intergranular cracking initiates.

TEM examinations on over aged samples showed the existence of long rows of precipitates that formed on curved lines (Fig. 4). It was further observed that a second type of precipitates with lozenge shape (Fig. 5) also formed which were more uniformly distributed compared to the ones observed on curved lines. An interesting feature of the lozenge shaped precipitates was that they appeared as rod-shaped particles when viewed at edge-on position, however, when inclined with respect to the electron beam their stepped edges could be noticed. These precipitates also displayed some strain field around them (Fig. 5a). EDS microanalysis presented in Table II and III revealed the presence of manganese inside the fine precipitates of both forms (precipitates on dislocations and plate precipitates) with lozenge shaped morphology.

In addition to the other two types intragranular precipitates very coarse $Mg_{12}Ce$ particles containing some internal linear defects were also observed (Fig. 5).

TABLE II EDS microanalysis of dislocation type small precipitates

	Mn	Ce	La	Nd	Pr
%wt	1.7	8	1.9	3.7	3.4

3 nm beam
The results are the average of 5 measurements.

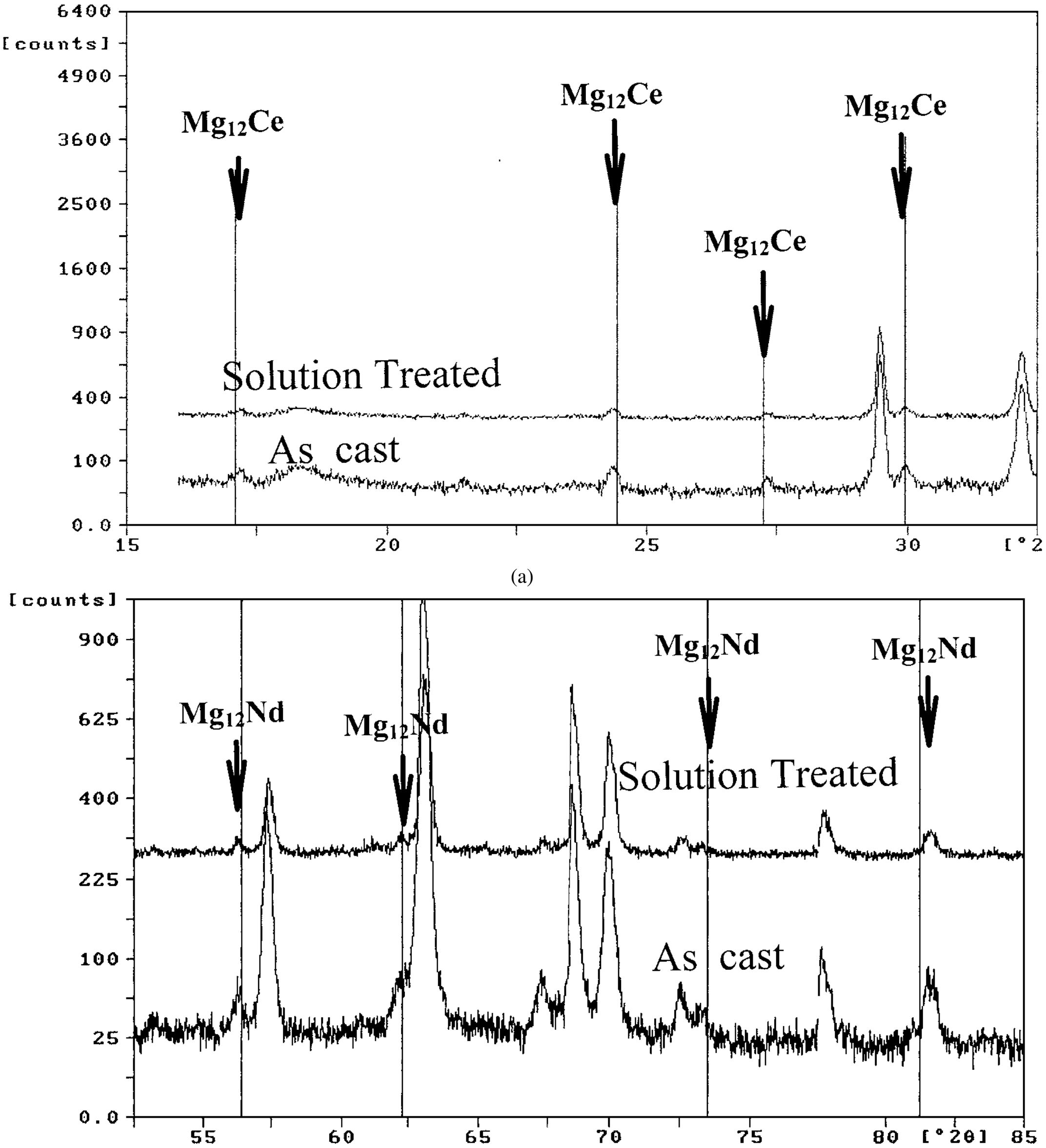

(a)

(b)

Figure 2 (a) X ray diffraction reaviling $Mg_{12}Ce$ peaks (alloy Mg-1.7-RE 0.3-Mn in the as cast and solution condition). (b) X ray diffraction reaviling $Mg_{12}Nd$ peaks (Alloy Mg-1.7-RE 0.3-Mn in the cast and solution condition).

TABLE III EDS microanalysis of plate type lozange shape small precipitates

	Mn	Ce	La	Nd	Pr
%wt	1.9	7.7	0.9	5.1	2.6

3 nm beam
The results are the average of 5 measurements.

Regardless of their size and morphology all types of precipitates were identified by electron diffraction patterns as $Mg_{12}Ce$ phase.

4. Mechanical properties

Age hardening response of the alloy was followed via microhardness measurements. The change in the

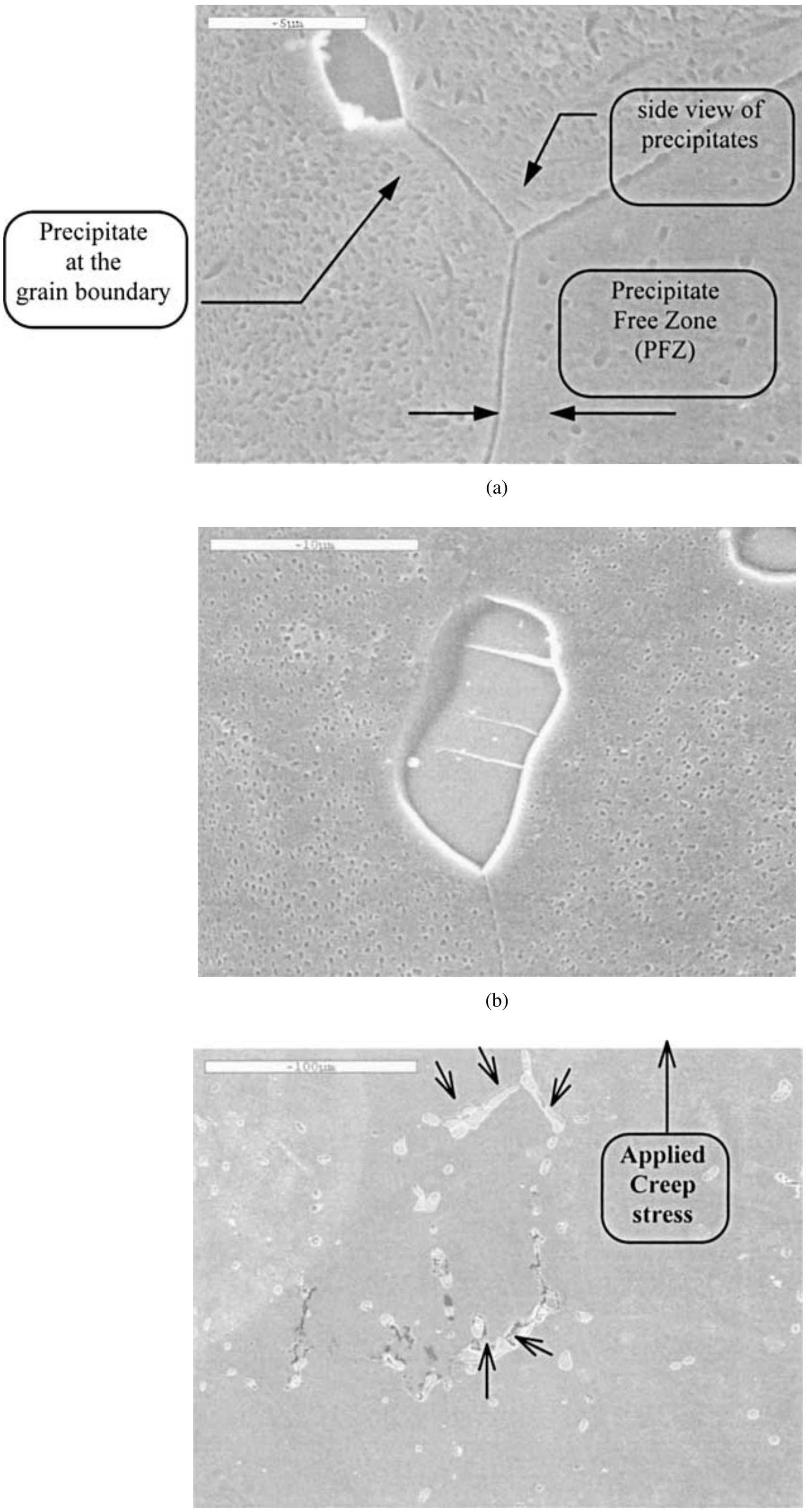

(a)

(b)

(c)

Figure 3 (a) Precipitate-free zones along the grain boundaries, (b) internally cracked $Mg_{12}Ce$ precipitate and (c) initiation of creep failure.

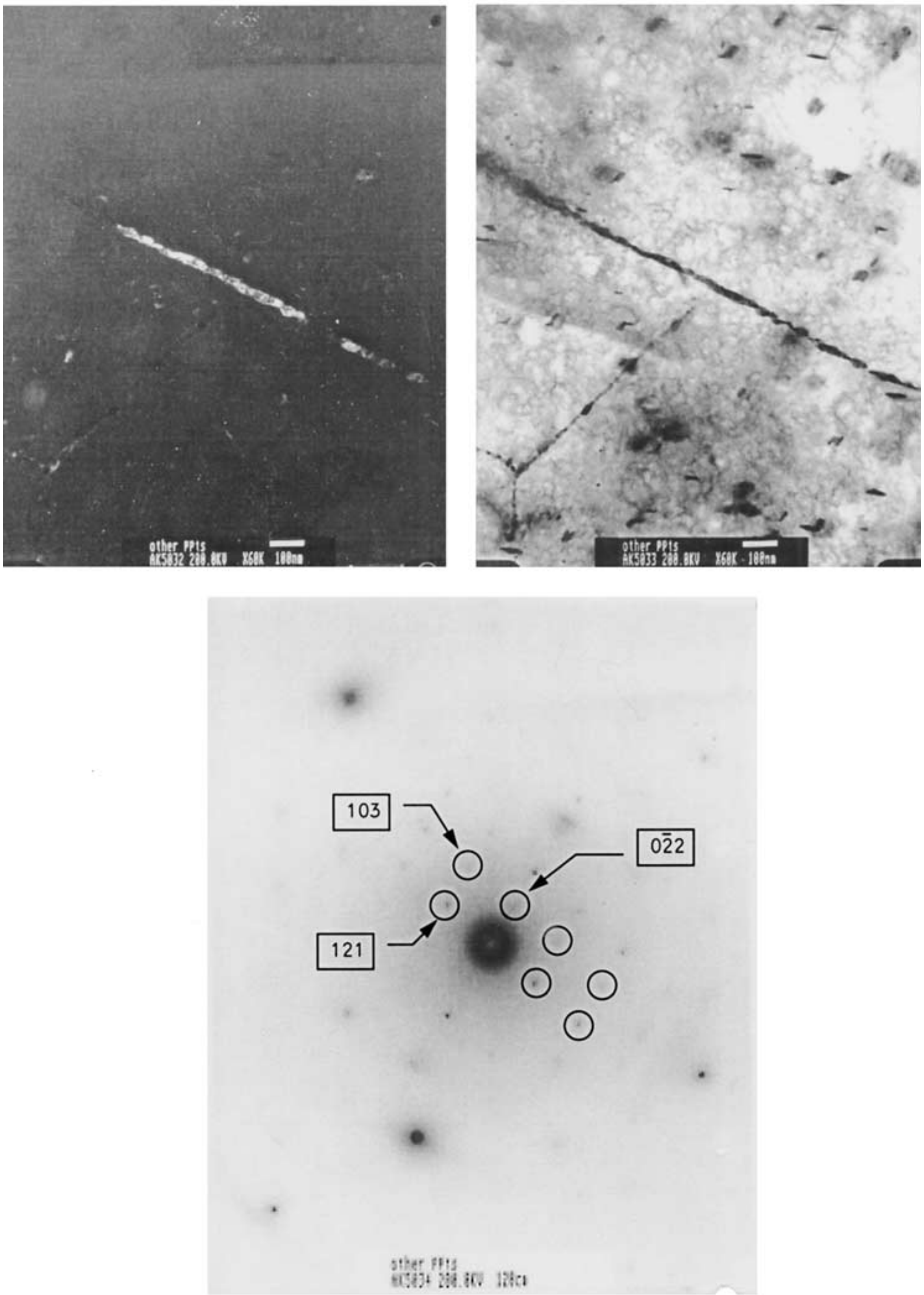

Diffraction pattern of the $Mg_{12}Ce$ equilibrium phase

Figure 4 (a) TEM—Identification of the precipitates on dislocations as $Mg_{12}Ce$ equilibrium phase and (b) Diffraction pattern of the $Mg_{12}Ce$ equilibrium phase.

microhardness of the alloy with ageing time is described in Fig. 7. It can be seen that the peak hardness is achieved in a few hours of aging time. Although the time to achieve peak hardness was unaffected, manganese addition appeared to have slightly increased the peak hardness of the alloy studied here as compared to the one containing only Ce addition. The compressive yield point at room temperature is presented in Fig. 8. It can be seen that when the alloy is peak aged (T6-condition) it has a slightly low compressive yield point when compared to AZ91D at the T6 condition.

The creep deformation of Mg-1.7RE(Ce)-0.3Mn alloy was assessed in the temperature range of 190 to 210°C, and in the stress range of 50–60 MPa. As shown in Fig. 9 a typical creep curve of the alloy consist of two stages, primary and secondary creep. The steady-state creep rate was calculated using the linear section of the curve as indicated in Fig. 9 and termed - secondary creep. The activation energy for the creep deformation was obtained by varying the temperature and calculating the steady-state creep rate at each step. The results are presented in Table IV. The activation energy was

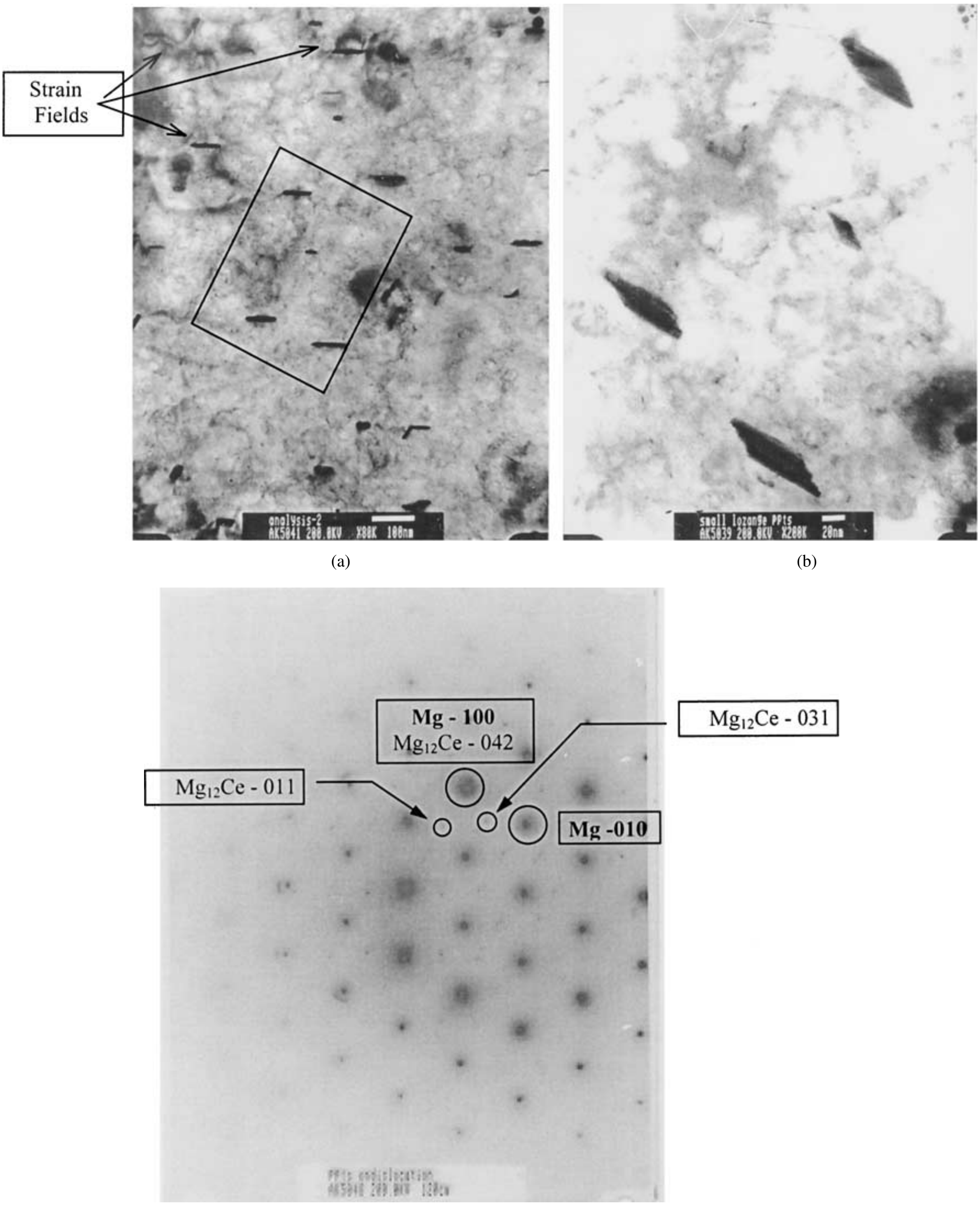

(a) (b)

(c)

Figure 5 TEM—Plate precipitates (Fig. 3.5b is the enlarged area of Fig. 3.5 a). (c) Diffraction pattern of the plate precipitates.

calculated using Equations 1 and 2 [6].

$$\dot{\varepsilon}_s = A\left(\frac{\sigma}{G}\right)^n e^{-\left(\frac{Q}{RT}\right)} \tag{1}$$

where A is the preexponential complex constant containing the frequency of vibration of the flow unit, the entropy change, and a factor that depends on the structure of the material, G is shear modulus of magnesium $G_T = 1.92{*}10^4 - 8.6T$ (where T is in kelvin); Q is activation energy; R is gas constant; and n is stress exponent constant.

$$Q = \frac{R\ln(\varepsilon_1/\varepsilon_2)}{(1/T_2 - 1/T_1)} \tag{2}$$

The activation energy was thus calculated from the creep rates at a varying temperature (Table IV) to be in the range of 240–252 KJ/mol.

An attempt was also made to calculate the stress exponent for the creep deformation at 190°C. In order to find the stress exponent the creep stress was varied and the steady-state creep rate was calculated at each

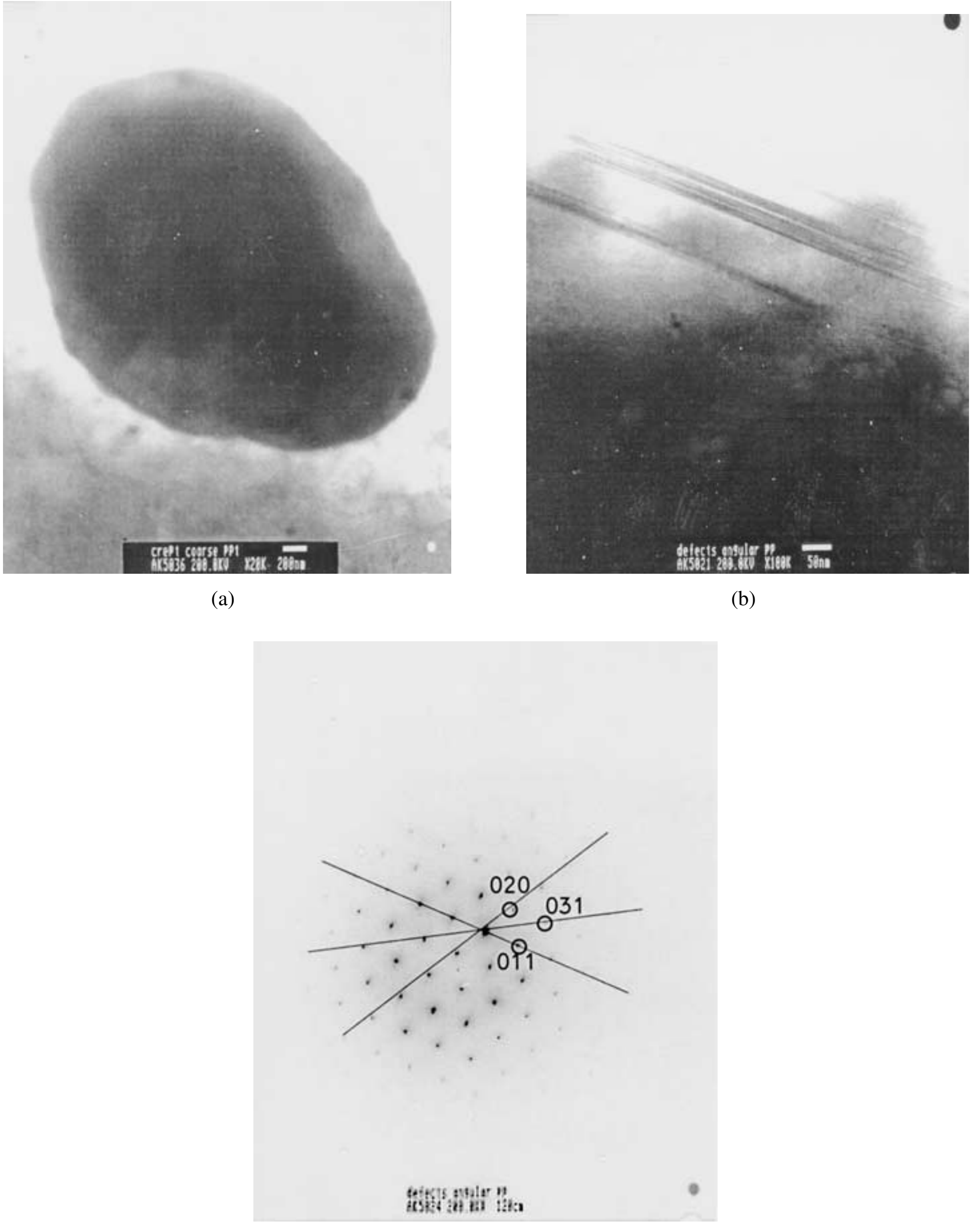

(a)

(b)

(c)

Figure 6 (a) Coarse $Mg_{12}Ce$ precipitate, (b) crystal fault of the $Mg_{12}Ce$, and (c) diffraction pattern.

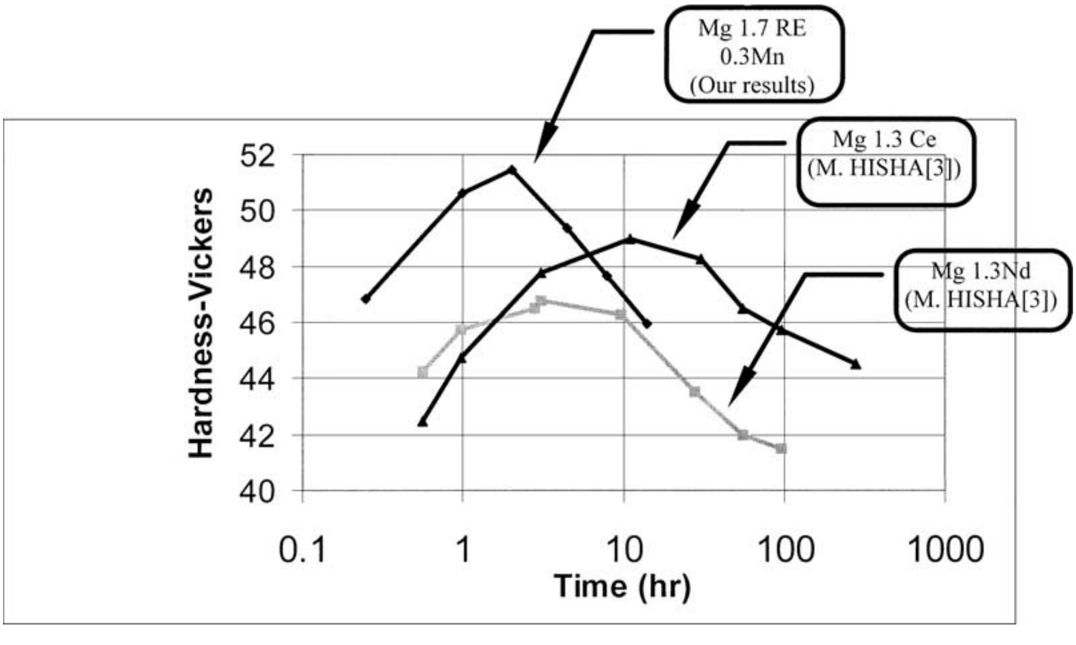

Figure 7 Age hardening of Mg 1.7%RE-0.3%Mn compared to Mg-Ce and Mg-Nd (3), alloys at 200 °C.

TABLE IV Variation of the steady creep rate versus temperature and stress

Temperature-°C	Minimum Creep Rate-%/hr Stress-50MPa	Minimum Creep Rate-%/hr Stress-55MPa
190	1E- 6	3E- 6
200	4E- 6	5E- 6
210		4E- 5

TABLE V Variation of the steady creep rate versuss stress

stress (MPa)	Creep rate sec-1
49.95	2.78E-10
55	1.11E-09
58.275	2.78E-09
60.55	3.89E-09

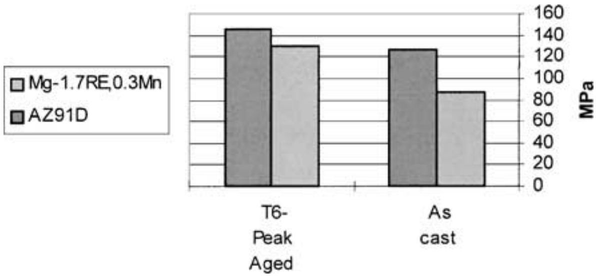

Figure 8 Compressive yield point of Mg 1.7%RE-0.3%Mn compared to AZ91D.

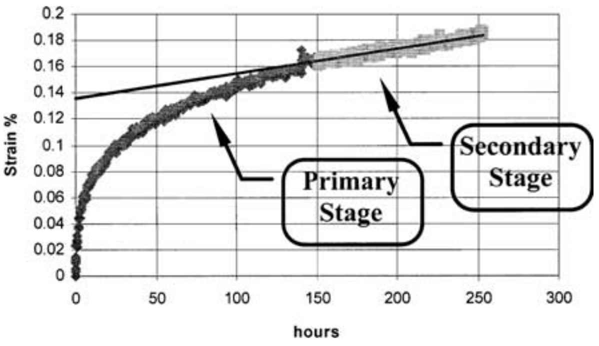

Figure 9 Typical creep curve of Mg 1.7%RE(Ce) 0.3%Mn at 190 °C/55 MPa.

step which resulted in the values given in Table V and Fig. 10. The stress exponent thus calculated was 14 as expressed in Fig. 10.

5. Discussion

The as-cast and the solution treated microstructures of the Mg-1.7RE-0.3Mn alloy resemble each other except for the grain morphologies. The as-cast structure is composed of broken dendrites while in the solution treated sample the dendritic grains no longer exist. The coarse grain boundary precipitates were not completely dissolved after solution treatment. This can be explained by the limited solubility of the RE elements in the α-magnesium matrix. It was shown that dissolved RE content led to the formation of some intragranular precipitates due to ageing during creep.

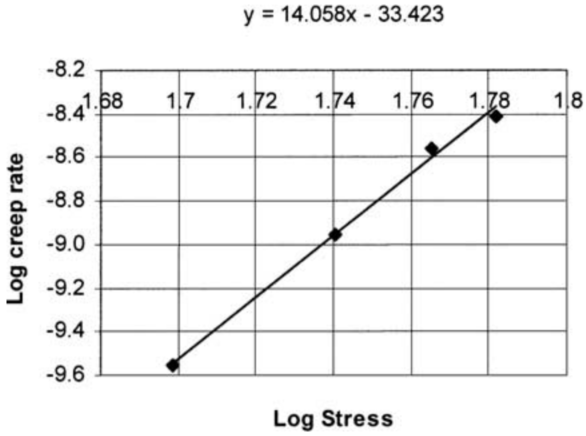

Figure 10 Stress exponent calculation.

Microstructural and microhardness observations suggested that by the time the steady state creep stage was reached (in Fig. 8 steady state creep began after 150 hr) the microstructure became overaged (over aging was reached after about 10 hr in Fig. 7). The creep resistance of the alloy studied is relatively high as can been seen in the comparison to other magnesium alloys presented in Fig. 11. This may be attributed to the fact that despite the overaged condition of the alloy most of the precipitates were still relatively fine.

The precipitates that appeared in rows probably formed on dislocations as the equilibrium precipitates during creep. These may have acted effectively to hinder the dislocation motion. The second type, termed as the lozenge shaped precipitates may have first precipitated as one of the metastable precursor, and then transformed into the equilibrium β phase. The sequence of such phase changes were previously observed on a similar alloy by L. Y. Wei *et al.* [2]. The observed changes in the microhardness of the alloy studied here may be taken to support this view as it is very similar to the one reported by M. Hisha *et al.* [3]. The stress field around the lozenge shaped precipitates may be indicating that these precipitates are also effective barriers to dislocation motion. The stepped edges on two parallel sides of the lozenge shaped precipitates is probably related to their growth mechanism, however, very difficult to explain on the basis of the available data.

The apparently good adherence between the grain boundary coarse precipitates and matrix may have contributed to the relatively high creep resistance of the material. It has been illustrated that these grain boundary precipitates did not separate from the matrix until internal cracking within them took place during creep (Fig. 3b).

The calculated activation energy for creep indicates that the creep mode involves a cross slip mechanism from basal to prismatic planes in the hexagonal crystal structure. Previous workers reported lower values (around 130 KJ/mol) when only basal slip was observed [7], and higher values of activation energy (around 220 KJ/mol) were calculated when cross slip took place [8].

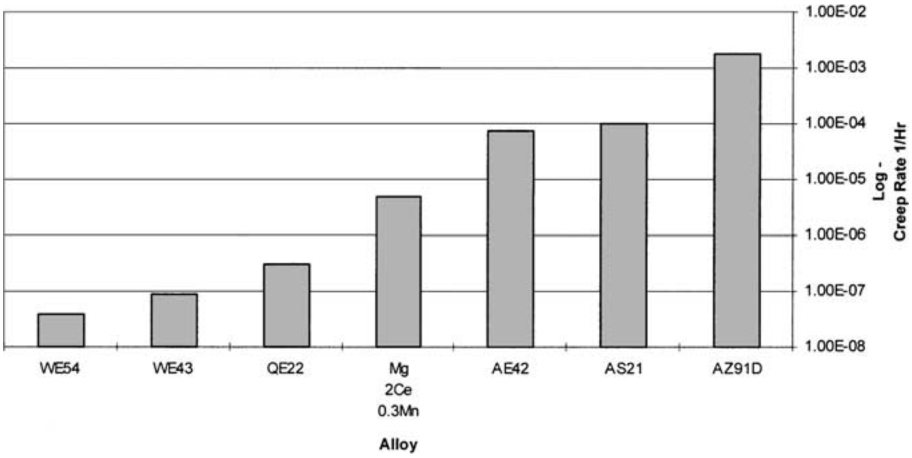

Figure 11 Steady state creep rates at 200°C, 55 MPa. The creep rates of WE54, WE43, QE22 and AZ91D are interplolated creep rates calculated by their activation energies and stress exponents.

6. Conclusions

1. Small addition of RE elements and manganese improved the creep resistance in comparison to commercial high temperature AE42 and AS21 alloys.

2. The microstructure in the over aged condition consisted of coarse grain boundary precipitates with good adherence to the surrounding grains, and fine intragranular equilibrium $Mg_{12}Ce$ precipitates in the form of rows along dislocation lines, and homogeneously dispersed lozenge shaped precipitates.

3. The fine intragranular equilibrium $Mg_{12}Ce$ precipitates in the form of rows along dislocation lines and the plate type are relatively rich in manganese.

4. The calculated activation energy for creep (240–250 KJ/mol) indicated that the creep mode involved cross slip of dislocations from basal to prismatic planes in the hexagonal crystal structure.

References

1. A. A. NAYEB and J. B. CLARCK, in "Phase Diagrams of Binary Magnesium Alloys" (1988) p. 78.
2. L. Y. WEI and G. L. DUNLOP, in "Mg Alloys and Their Applications"—Conf., Garmisch-Partenkirchen, Germany, April 1992, p. 335.
3. M. HISHA, J. C. BARRY and G. L. DUNLOP, in Proceedings of the Third International Magnesium Conference, Manchester, UK, April 1996, p. 369.
4. T. F. MELLOR, *Trans. AIME* **191** (1951) 987.
5. G. A. MELLOR and R. RIDLEY, *J. Inst. Met.* **88** (1948–49) 417; Ahmed , R. Pilkington "Mg Alloys and Their Applications"—Conf., Garmisch-Partenkirchen, Germany, April 1992, p. 251.
6. G. E. DIETER, "Mechanical Metallurgy" (1988) p. 451.
7. VAGARALI and LANGDON, *Acta Metall.* **29** (1983) 1969.
8. H. KARIMZADEH, J. M. WORRALL, R. PILKINGTON and G. W. LORIMER, "Tensile and Creep Fracture of a Mg-Y-Re Alloy" (Magnesium Technology, Inst. of Metals, London, 1987) p. 138.
9. K. MILICA, J. CADECK and P. RYS, *Acta. Metall.* **18** (1970) 1071.
10. M. AHMED, "Mg Alloys and Their Applications"—Conf., Garmisch-Partenkirchen, Germany, April 1992, p. 251.

Received 24 November
and accepted 28 December 1999